

O/W Pickering emulsions stabilized by cocoa powder: role of the emulsification process and of composition parameters

Cécile Joseph^{a,b,c}, Raphaëlle Savoie^{a,b,c}, Christelle Harscoat-Schiavo^{a,b,c}, Didier Pintori^d,

Julien Montell^{a,b,c}, Fernando Leal-Calderon^{a,b,c}, Chrystel Faure^{a,b,c}*

^a Univ. Bordeaux, CBMN, UMR 5248, 33600 Pessac, France

^b CNRS, CBMN, UMR 5248, 33600 Pessac, France

^c Bordeaux INP, CBMN, UMR 5248, 33600 Pessac, France

^d ITERG, 33600 Pessac, France

*Corresponding author: Chrystel Faure

e-mail: chrystel.faure@enscbp.fr, phone number: 00 (33) 540006833, fax number: 00 (33)

54008496

ABSTRACT

We fabricated oil-in-water emulsions stabilized by delipidated commercial cocoa powder. The emulsions were characterized in terms of droplets and particles size distribution and interfacial coverage by cocoa powder by developing methods to separate droplets from adsorbed and unadsorbed cocoa particles. Three different processes were compared for their ability to produce fine and stable emulsions: rotor/stator turbulent mixing, sonication and microfluidization. Among those techniques, microfluidization was the most performing one. In this case, micron-sized emulsions with narrow size distributions could be obtained with more than 90 wt.% of the powder insoluble material anchored to the interfaces, and they were still stable after 90 days. It was demonstrated that the mixing process did not generate finer cocoa particles but provoked disentanglement of the large primary particles, providing them an open, expanded structure that facilitated emulsification. It was also shown that the finer insoluble fraction of the powder and the soluble fraction had no significant impact on emulsification and on kinetic stability. In the poor particles regime, the oil-water interfacial area varied linearly with the amount of adsorbed powder, suggesting that the final droplet size was controlled by the so-called limited coalescence process, as already observed in conventional Pickering emulsions stabilized by spherical solid particles.

Keywords: Cocoa powder; solid particles; Pickering emulsions; microfluidization; limited coalescence

1. Introduction

Emulsions are metastable systems generally obtained in the presence of different surface-active species like surfactants, amphiphilic polymers or proteins. It is now well established that solid amphiphilic particles can kinetically stabilize emulsions. Solid-stabilized emulsions were first observed by Ramsden and Pickering (Pickering, 1907; Ramsden, 1903) and are commonly named “Pickering emulsions”. Some general rules governing the behavior of such materials could be inferred from studies based on model mineral or organic spherical particles (Arditty, Whitby, Binks, Schmitt, & Leal-Calderon, 2003; Ashby & Binks, 2000; Binks, 2017; Golemanov, Tcholakova, Kralchevsky, Ananthapadmanabhan, & Lips, 2006; S. Tcholakova, D. Denkov, & Lips, 2008). Outstanding properties in terms of kinetic stability and rheology were obtained in most cases owing to the formation of a dense and rigid interfacial layer. Solid particles are irreversibly anchored at the oil–water interface unlike surfactant molecules, which adsorb and desorb within very short time scales under the effect of thermal fluctuations (Binks, 2002). To adsorb at the interface, particles are required to be wet by both liquids. Following the empirical Finkle’s rule (Finkle, Draper, & Hildebrand, 1923), the emulsion type (oil-in-water (O/W) or water-in-oil (W/O)) is mainly determined by the relative particle wettability in both liquids: the continuous phase of the preferred emulsion is normally the one in which the particles are preferentially dispersed. Indeed, the continuous phase of an emulsion stabilized by particles having a high degree of hydrophilicity will be the water phase, whereas hydrophobic particles will preferentially stabilize water drops dispersed in oil.

It has been demonstrated that highly monodisperse Pickering emulsions can be easily obtained following the limited coalescence process (Arditty et al., 2003; Whitesides & Ross, 1995). It consists in producing a large excess of oil–water interface compared to the amount that can be covered by the solid particles. To favor this process, the emulsions have to be formulated in the presence of a small amount of solid particles. When the agitation is stopped, the partially unprotected droplets coalesce, thus reducing the total oil–water interfacial area. Since the particles are irreversibly adsorbed, coalescence stops as soon as

the droplets interface is sufficiently covered. The limited coalescence process is a fast and versatile process allowing the production of stabilized monodisperse emulsions whose average diameter usually ranges from 1 μm to 1 cm (Arditty et al., 2003).

The application field of Pickering emulsions is widespread, emulsions being used either as intermediate or end products. Pickering emulsions based on solid food-grade particles are of great interest in the food arena. Using these biomass-based particles to fabricate emulsions meets indeed consumers' requirements by replacing synthetic surface-active agents with environmentally friendly compounds. Food-grade particles notably include fat and wax crystals, starches (Yusoff & Murray, 2011), chitin nanocrystals, cellulose fibers or nanocrystals (Campbell, Holt, Stoyanov, & Paunov, 2008; Sarkar, Li, Cray, & Boxall, 2018; Sarkar, Zhang, Murray, Russell, & Boxal, 2017) flavonoids (Luo et al., 2011) and protein microgels or nanoparticles (Destribats, Rouvet, Gehin-Delval, Schmitt, & Binks, 2014; Sarkar et al., 2016; Shao & Tang, 2016).

The present work focuses on the stabilization of emulsions by cocoa powder. Cocoa beans are the seeds of the *Theobroma cacao* tree. The contents of the cocoa beans are ground to produce cocoa paste (mass), which is composed of particles and cocoa butter. The cocoa paste is crushed by a hydraulic press to separate cocoa butter from cocoa paste, leaving a cocoa press cake. This latter is ground to produce cocoa powder. The process can be adapted to modify powders compositions and levels of fat. Cocoa powder, typically contains a variety of bio-compounds, such as phenolics, hydrocolloids, sugars, proteins, fibers, theobromine and 10-25% lipids with a chemical profile similar to that of cocoa butter (Lecumberri et al., 2007; Zak & Keeney, 1976). It serves in the food industry for a variety of applications such as confectionery, bakery, frozen desserts and beverages. Gould *et al.* (Gould, Vieira, & Wolf, 2013) explored the functionality of cocoa particles as emulsion stabilizers through the mechanism of Pickering stabilization. All emulsions were prepared using a high shear overhead mixer giving rise to rather coarse emulsions. Several cocoa sources (cocoa powders, cocoa fiber and cocoa mass) were evaluated. All showed ability to

form kinetically stable O/W emulsions except cocoa mass, which was explained by the lower solids content. It was suggested that the fine fraction of the powders adsorbs at the oil droplet interfaces whereas larger particles play a role in structuring the aqueous phase surrounding the droplets.

Following the seminal study of Gould *et al.*, the work related in this article aims at gaining deeper understanding about the main factors controlling the droplets size distribution and stability of O/W solid stabilized emulsions prepared from sunflower oil, water, and cocoa powder. Since cocoa powders comprise soluble and insoluble fractions, the influence of each fraction on emulsion properties was investigated. Moreover, particles (insoluble fraction) are polydisperse, shapeless and potentially fragmentable and/or deformable under shear. Thus, the emulsification ability is potentially dependent on the emulsification process. We then examine the effect of three different emulsification processes -rotor/stator turbulent mixing (high speed overhead mixing), sonication and microfluidization- on particle size and consequently its effect on adsorption efficiency and droplet size. Eventually, the influence of particles and oil concentrations on the initial average droplet size and on the kinetic evolution of the emulsions was studied focusing on the low particle concentration regime to see whether emulsions with narrow size distributions can be obtained through limited coalescence.

2. Materials and methods

2.1. Materials

The oil phase of the emulsions consisted of commercially available sunflower oil (Rustica, France, density: 0.92 g.cm^{-3}) purchased from a local supermarket. Cocoa powder from VanHouten (France) was used to stabilize the emulsions. Its processing is described in section 2.2. . It contained 22 wt.% lipids (extraction with hexane according to NF EN ISO 734-1) and its ash content after calcination was 8.6 wt.% (10.5 wt.% of the delipidated powder, determined gravimetrically according to NF ISO 6884). The aqueous phase was

buffered (pH=7) using a 0.1 mol.L⁻¹ mixture of dipotassium phosphate and monopotassium phosphate (Sigma-Aldrich, France). Sodium dodecyl sulfate (SDS) (Sigma-Aldrich, France) was used to desorb cocoa particles from the oil-water interfaces for droplet size measurements. The water used in the experiments was deionized with a resistivity close to 15 MΩ.cm at 20 °C. Sodium azide was added at 0.1 wt.% in all aqueous phases as a preservative to avoid any bacteriological growth that would have modified the composition of the system and would have compromised our interpretations

2.2. *Powder processing*

The cocoa powder was delipidated with hexane according to NF EN ISO 734-1 standard, milled with a high-speed centrifugal rotor mill (ZM-200, Retsch, Poland, rotational speed at 31-93 m.s⁻¹) and sieved through a 120 µm aperture mesh. For emulsions fabricated via microfluidization, the resulting powder was used either directly or after further intense milling. In this latter case, the powder was dispersed in deionized water at 5 wt.% and processed using a bead mill (Dyno[®]-Mill Multi Lab, Willy A Bachofen-WAB, France), equipped with chrome accelerators (DYNO-Accelerators, Willy A Bachofen-WAB, France). The grinding chamber (0.6L) was previously filled with water and 0.8 mm zirconium beads (Zyrmill Y, Willy A Bachofen-WAB, France) at the maximum level of bead filling (65% v/v). Milling was run in continuous mode in one single pass. The dispersion was pumped at a flow rate of 0.1 kg.min⁻¹ with a rotational speed for the grinding media of 10 m.s⁻¹. Dispersion was cooled with water circulating in the jacket of the grinding chamber. The milled dispersion was then freeze-dried by zeodratation (Bucher, Drytech, Switzerland) at 30 °C and 1 mbar for 24h in order to obtain dried cocoa powder.

2.3. *Emulsion preparation*

All powder concentrations refer to the aqueous phase (from 0.5 to 12 wt.%) and oil contents refer to the whole emulsion (from 10 to 50 wt.%). A table gathering the compositions of all samples discussed in this article is provided in supplementary information (SI.1). The emulsions batches had a total mass of 20 g. The pH of the aqueous phase was

set at 7 by means of the phosphate buffer (0.1 mol.L^{-1}). Three emulsification techniques were implemented. (i) High speed overhead mixing: the processed cocoa powder was dispersed in the buffered aqueous phase at the appropriate concentration with a magnetic stirrer for 20 min. The powder was further dispersed using an Ultra-Turrax® mixer (rotor-stator system, T25 digital, dispersing element S25 N-25F, IKA, Germany) working at 6 000 rpm for 2 min. The stirring speed was then increased up to 8 000 rpm and the required amount of sunflower oil was slowly added to the water phase under agitation (around 2 min). Mixing was then extended for 10 min at 12 000 rpm. (ii) Ultrasounds: the processed cocoa powder, the buffered aqueous phase and sunflower oil were added in this order and mixed under manual stirring. A 5 mm-ultrasonic probe (Tapered Microtip, Branson, France) was immersed in the blend just after manual stirring. Ultrasounds were applied (Converter 102C and Sonifier 250, Branson, France) for 5 min, at 10 W and 80% of duty cycle. (iii) Microfluidization: a pre-emulsion was first obtained with the Ultra-turrax® device following the method previously mentioned. The system was then homogenized at high pressure (800 bars unless otherwise specified) using a microfluidizer (Microfluidizer M-110S, USA) fitted with a Y-single slotted chamber and an internal $75 \mu\text{m}$ air-gap. The whole emulsion volume was submitted to 6 passes through the homogenizing chamber.

Emulsions were stored for several weeks at $4 \text{ }^\circ\text{C}$ after fabrication.

2.4. *Analysis of soluble compounds*

Hereafter, the term “particles” will refer to the water-insoluble fraction of the powder. Being denser than water, such fraction can be separated from the soluble one upon centrifugation.

A 10 wt.% dispersion of delipidated cocoa powder in deionized water (dispersion with a magnetic stirrer for 20 min) was centrifuged for 1h at $100\,000 \text{ g}$ (g being the earth gravity constant) (Aventi J-301 Centrifuge, Beckman Coulter, USA). The supernatant containing the soluble fraction was collected and freeze-dried for mass measurement. The same procedure was performed on a 10 wt.% dispersion of cocoa powder processed in the microfluidizer at

800 bars (6 passes). Emulsions were also centrifuged 1h at 100 000 g, in order to induce particles sedimentation and droplets creaming. The intermediate aqueous phases were carefully sampled and centrifuged a second time for 5 min at 4 600 g to remove residual droplets before freeze drying.

After re-dissolution of the freeze-dried phases, water-soluble carbohydrates, proteins and polyphenols were quantified. Carbohydrates were titrated using the anthrone-sulfuric acid assay (Leyva et al., 2008). Briefly, carbohydrates were hydrolyzed (150 μL of reagent at 1 $\text{g}\cdot\text{L}^{-1}$ for 50 μL of sample, 30 s of stirring, 20 min at 100 $^{\circ}\text{C}$) and the resulting furfuralic compounds were assayed at 620 nm using a glucose calibration curve from 0 to 100 $\text{mg}\cdot\text{L}^{-1}$. Proteins were quantified using Bradford reagent (or Coomassie brilliant Blue) (150 μL for 5 μL of sample), which is known to form light-absorbing complexes in the presence of proteins. Complexes were titrated at 595 nm using a Bovine Serum Albumin (BSA) calibration curve from 0 to 500 $\text{mg}\cdot\text{L}^{-1}$ (J. E. Noble & Bailey, 2009). Polyphenols were quantified using Folin-Ciocalteu reagent (100 μL for 20 μL of sample and 80 μL of 75 $\text{g}\cdot\text{L}^{-1}$ sodium carbonate aqueous solution). This yellow-colored acid turns to blue upon phenol oxidation. Polyphenol quantification was performed using a gallic acid calibration curve from 0 to 100 $\text{mg}\cdot\text{L}^{-1}$ (Zhang et al., 2006).

2.5. *Microscopy*

An Olympus BX51 optical microscope (Olympus, Japan) fitted with a digital color camera (Color View, Olympus, Japan) was used to observe cocoa particles and emulsions. To facilitate the observation, emulsions and particle dispersions were always diluted (200 μL of dispersion/emulsion in 1 500 μL of deionized water). Samples were deposited on a glass slide and were covered by a cover slip. A specific configuration was adopted in order to avoid sample damage. Indeed, we observed that the shear applied upon spreading of the confined liquid sometimes provoked droplet coalescence on the glass substrate. To avoid this phenomenon, cavity microscopy slides (well slides) with single ground and polished spherical

cavities (Marienfeld, Germany) were adopted for observations. Samples were placed in the cavity zone before the cover slip was carefully deposited.

Particles could be visualized owing to their self-fluorescent properties. A Leica DMI 600B fluorescence microscope equipped with a DFC350 FX camera (Leica Microsystems, Germany) was used to this end. A filter cube N3 (Leica, Germany) with an excitation wavelength around 546 nm and an emission wavelength around 600 nm was used. In order to remove free particles from the continuous phase, and to visualize only adsorbed particles onto the oil droplets, the emulsions were washed before observation. They were diluted and submitted to gentle centrifugation at 2 000 g for 2 min using a C-1200 26 joules centrifuge (Labnet, Korea) to separate free particles (sediment) from the particles-covered oil droplets (cream). The cream was removed, and diluted with the phosphate buffer before being centrifuged once again under the same conditions. The resulting cream was observed after dilution.

2.6. Particle size measurements

Particle size distributions were measured using a Mastersizer 2000 apparatus (Malvern Instruments, UK). Static light scattering data were transformed into size distribution using Fraunhofer theory and the irregular mode to account for the non-spherical shape of the particles. Despite its limitations, Fraunhofer theory was chosen mainly because it does not require knowledge of the optical indexes of the dispersed phase (neither the refractive index nor the absorption index of cocoa are documented in the literature). A small volume of sample was introduced under stirring (1 600 rpm) in the dispersion unit containing deionized water. Each measurement was performed in triplicate. The particles distributions were characterized by their volume-averaged diameter, D_v , defined as:

$$D_v = \frac{\sum N_i D_i^4}{\sum N_i D_i^3} \quad (1)$$

where N_i is the total number of particles with diameter D_i .

The finest fraction of particles was examined specifically (see section 3.4). The fraction that did not undergo natural sedimentation over 24h of storage was analyzed at 20 °C by

dynamic light scattering (DLS) using the Vasco particle size analyzer (Cordouan Technologies Ltd, Pessac, France). The detection angle of 135° was large enough to ensure that the signal was not disturbed by multiple scattering. The autocorrelation functions were measured and the Z-average hydrodynamic diameters were calculated using the cumulant method (Berne & Pecora, 1976). Each measurement was an average of 6 repetitions of 180 s. All analyses were performed with the software supplied by the manufacturer.

2.7. Droplet size measurements

The size distributions were measured using the Mastersizer 2000 apparatus. Static light scattering data were transformed into size distribution using Mie Theory. The droplet refractive index was 1.47 and that of the aqueous phase was 1.33. A small volume of sample was introduced under stirring (1 600 rpm) in the dispersion unit containing a solution of SDS at 0.2 wt.%. Each measurement was performed in triplicate. Samples that underwent creaming were manually agitated in order to restore homogeneity to ensure a representative size distribution. The droplets distributions were described in terms of their volume-averaged diameter, D_v (Eq. (1)), surface-averaged diameter, D_s , and polydispersity, P , defined as:

$$D_s = \frac{\sum N_i D_i^3}{\sum N_i D_i^2}, P = \frac{1}{\bar{D}} \frac{\sum N_i D_i^3 (\bar{D} - D_i)}{\sum N_i D_i^3} \quad (2)$$

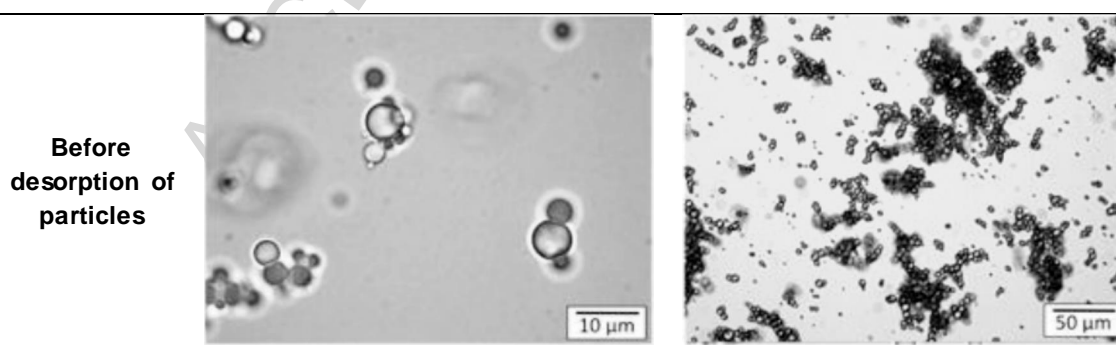
The median diameter, \bar{D} , is the value for which the cumulative undersized volume fraction is equal to 50%.

Measurements based on light-scattering were made difficult in this study because emulsification resulted in droplets aggregation, whatever the process, and because particles were hardly distinguishable from droplets. A protocol was thus developed to get rid of cocoa particles present both in the bulk phase and at the oil/water interface. In order to desorb cocoa particles, emulsions were treated with SDS which is a surface-active species. The emulsions were submitted to a 4-fold dilution in a 10 wt.% SDS solution. The system was then gently stirred with a magnetic bar for 10h. The emulsions diluted in the SDS solution were then centrifuged for 5 minutes at 220 g (Rotanta 460 RF Centrifuge, Hettich Lab Technology, Germany) in order to separate the particles (sediment) from the oil droplets

(cream). The resulting creams were milky and colorless (not brownish) (see supplementary information, SI.2), suggesting that cocoa particles were not present anymore. The creams were collected, diluted 50 times in deionized water and analyzed.

SDS has the ability to adsorb at the oil-water interface and to displace the particles from it. This low molecular weight surfactant is also known to displace species with high interfacial adsorption energies like proteins (Mackie, Gunning, Wilde, & Morris, 2000; Pradines, Krägel, Fainerman, & Miller, 2008). An illustration is given in Fig. 1 for emulsions containing 4 wt.% of cocoa powder in the aqueous phase and 20 wt.% sunflower oil, fabricated by microfluidization at 800 bars. As evidenced in the microscope images, SDS treatment led to droplets separation. The emulsions were also observed by fluorescence microscopy and particles were not detected anymore at the interfaces. In the absence of fluorescence signal emanating from the particles, the images were totally black. This proved that particles were totally desorbed after SDS treatment. Moreover, the droplets sizes were apparently preserved.

The repeatability of the method was also evaluated by sampling 3 times the same emulsion and analyzing the size distributions, each value being a mean of 3 repetitions of the same sample. An example is given in Table 1. The method implemented to desorb particles and to measure the droplet size by static light-scattering was repeatable, as the standard deviations were always reasonably low.



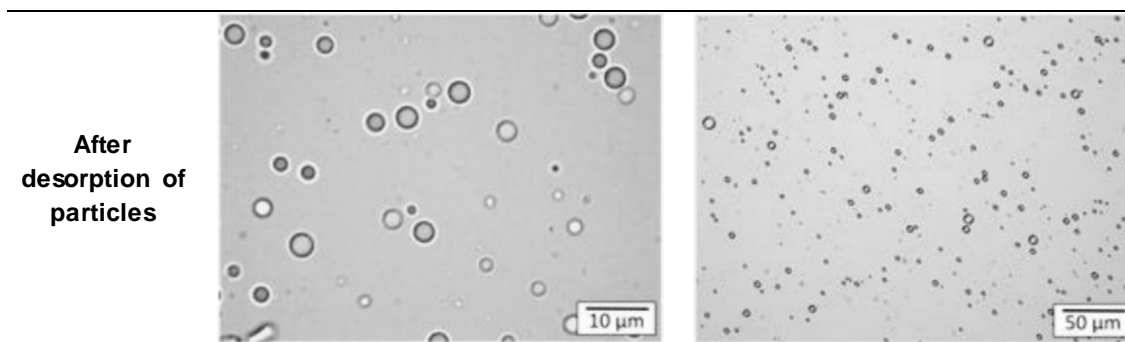


Figure 1

Table 1: Size data of an emulsion fabricated by microfluidization (800 bars) composed of 4wt. % cocoa particles and 20 wt.% sunflower oil.

	D_v (μm)	D_s (μm)	P
Sample 1	3.89	3.18	0.39
Sample 2	3.88	3.19	0.37
Sample 3	3.96	3.23	0.39
Mean	3.91	3.20	0.38
Standard deviation	0.05	0.03	0.01

2.8. Anchoring ratio

We defined the anchoring ratio (or adsorption efficiency) as the percentage of particles attached to the droplets, relative to the total particles content:

$$\text{Anchoring ratio (\%)} = 100 \times \frac{m_p^i - m_p^f}{m_p^i} \quad (3)$$

where m_p^f is the mass of free particles and m_p^i is the total mass of particles, *i.e* the mass of insoluble powder. Following the measurements of section 3.3.1, this latter was estimated as $m_p^i \approx 0.8 \times m_p$, where m_p is the total mass of cocoa powder. The pertinence of the anchoring ratio defined according to Eq. (3) is justified by the fact that the soluble fraction did not exhibit any apparent functionality. This issue will be developed in section 3.3.

In order to quantify m_p^f , the droplets were separated from the aqueous phase containing free (i.e. non-adsorbed) particles. Since the application of a centrifugal field can provoke partial desorption of the particles (Leclercq et al., 2012), cocoa-stabilized emulsions were first diluted 10 times with deionized water to reduce their overall viscosity, and stored for two days to allow natural creaming. The cream was removed, diluted 10 times and stored for two days again. Both subnatant phases, containing free particles, were gathered. In order to remove the residual oil droplets that did not cream naturally because of their small size, several centrifugations (Rotanta 460 RF Centrifuge, Hettich Lab Technology, Germany) with increasing rotation speeds were performed for 5 min at 20 g, 100 g, 1 000 g, 7 000 g, 14 000 g, 17 000 g and 10 min at 17 000 g. The rotation speed was increased progressively to minimize the risk of particle desorption from the residual droplets. At each stage, three phases could be distinguished in the centrifuge tubes: a thin creamed layer, an intermediate slightly turbid and colored aqueous phase containing the soluble fraction, and a particles sediment. The cream was removed after each centrifugation step, and replaced by deionized water to keep the total volume constant. After the last centrifugation step, no cream was observed in the sample and the upper phase was fully transparent, reflecting the absence of droplets. This latter phase was replaced by water to remove soluble compounds. After redispersing the sediment, the sample was freeze-dried (Bucher, Drytech, Switzerland) and weighted to finally obtain the mass of free particles.

3. Results and discussion

3.1. Influence of the emulsification process on cocoa particles

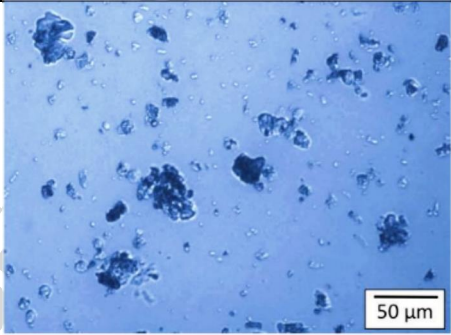
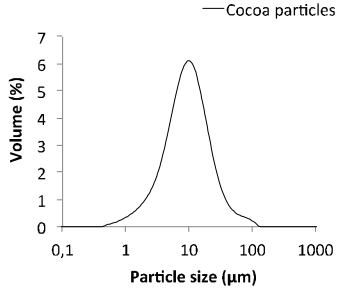
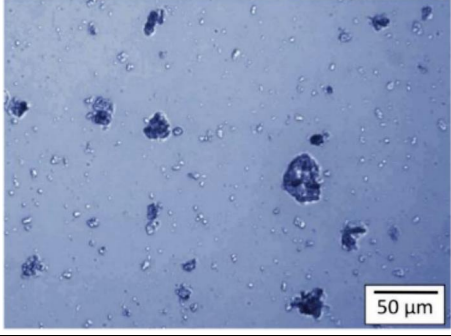
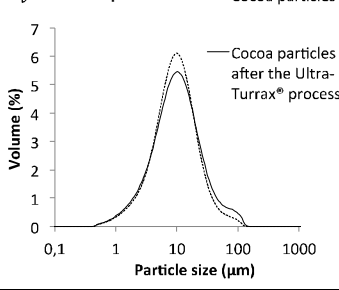
As particle size is known to be an influencing parameter in Pickering emulsions (Binks & Lumsdon, 2001), the impact of the emulsification process on the size of cocoa particles was investigated. For that purpose, dispersions of 5 wt.% delipidated cocoa powder were submitted to the same mechanical treatments as those adopted for emulsification (section 2.3), i.e. rotor/stator turbulent mixing (Ultra-Turrax®), sonication, microfluidization at 800 bars

and bead-milling. The corresponding size distributions were measured following the method described in section 2.6. Characteristic microscope images and size distributions are given in Fig. 2. Data include the unprocessed sample given as a reference. The unprocessed powder comprises micron-sized particles, as well as large shapeless particles with a characteristic size around 14 μm . Interestingly, large particles ($\geq 10 \mu\text{m}$) appear as dark-brown, light absorbing objects, indicating they are dense and thick. The powder submitted to Ultra-Turrax® mixing has features similar to the initial one. This treatment had no real impact on the size distribution of the cocoa particles as well as on their microscopic appearance. However, compared to the initial powder, the mean peak in the distributions resulting from sonication, microfluidization and bead-milling is shifted towards larger sizes. This evolution suggests that the large particles have a more open structure than the dense non-processed ones. This is confirmed by the microscope images showing highly anisotropic, less dense and thinner objects. In this case, it is likely that the mixing intensity was high enough to disentangle the large primary particles, providing them an open, expanded structure. A processed dispersion confined between two microscope glass slides was sheared by submitting the cover slip to a back and forth translation. Fig. 3 reveals that large particles tended to roll up in the direction perpendicular to the applied shear. This observation can be interpreted considering that large particles in processed samples behave pretty much like flat deformable membranes (see image of Fig. 3). We checked that such particles did not result from the aggregation of smaller ones. Firstly, we did not observe any particle breakup or disintegration upon shearing but rather their winding, as revealed by Fig. 3. Secondly, the mixing intensity of the dispersing unit of the Mastersizer 2000 apparatus was varied and the size distribution remained invariant. Eventually, measurements were carried out using a 0.2 wt% SDS solution in the dispersion unit in an attempt to disaggregate clusters, but the results were identical to those obtained with deionized water.

We are aware that the optical model (Fraunhofer) used in this study is only valid for scatterers whose size is larger than several micrometers. It cannot be excluded that the high mixing intensity of the different mechanical treatments generated fragments in the micron or

submicron range that were not correctly accounted for by the model. To quantify the fraction of fine particles, suspensions deriving from each mechanical treatment were allowed to sediment for 24 hours. At least 70 wt.% of the cocoa powder was collected in the sediments, irrespective of the treatment. Thus, the fraction of Brownian particles never exceeded 10 wt.% of the total cocoa mass, considering that the soluble compounds represent 20 wt.% of the whole cocoa powder (see section 3.3.1). The average size of this population measured by DLS was 1.35 μm for cocoa dispersions submitted to microfluidization at 800 bars.

From this set of experiments, we conclude that the mechanical treatment imposed by the emulsification process does not produce significant particles break up but has a noticeable impact on the structure of cocoa particles. Except rotor-stator turbulent mixing, all treatments tend to disentangle large particles, which likely increases their specific surface area and thus their capacity to attach oil droplets. Differences in terms of emulsifying properties of the powder are thus to be expected depending on the adopted technique.

Particles	Microscopic observations	Size distribution and D_v
Without any process		$D_v = 13.8 \mu\text{m}$ 
After the Ultra-Turrax® treatment		$D_v = 15.9 \mu\text{m}$ 

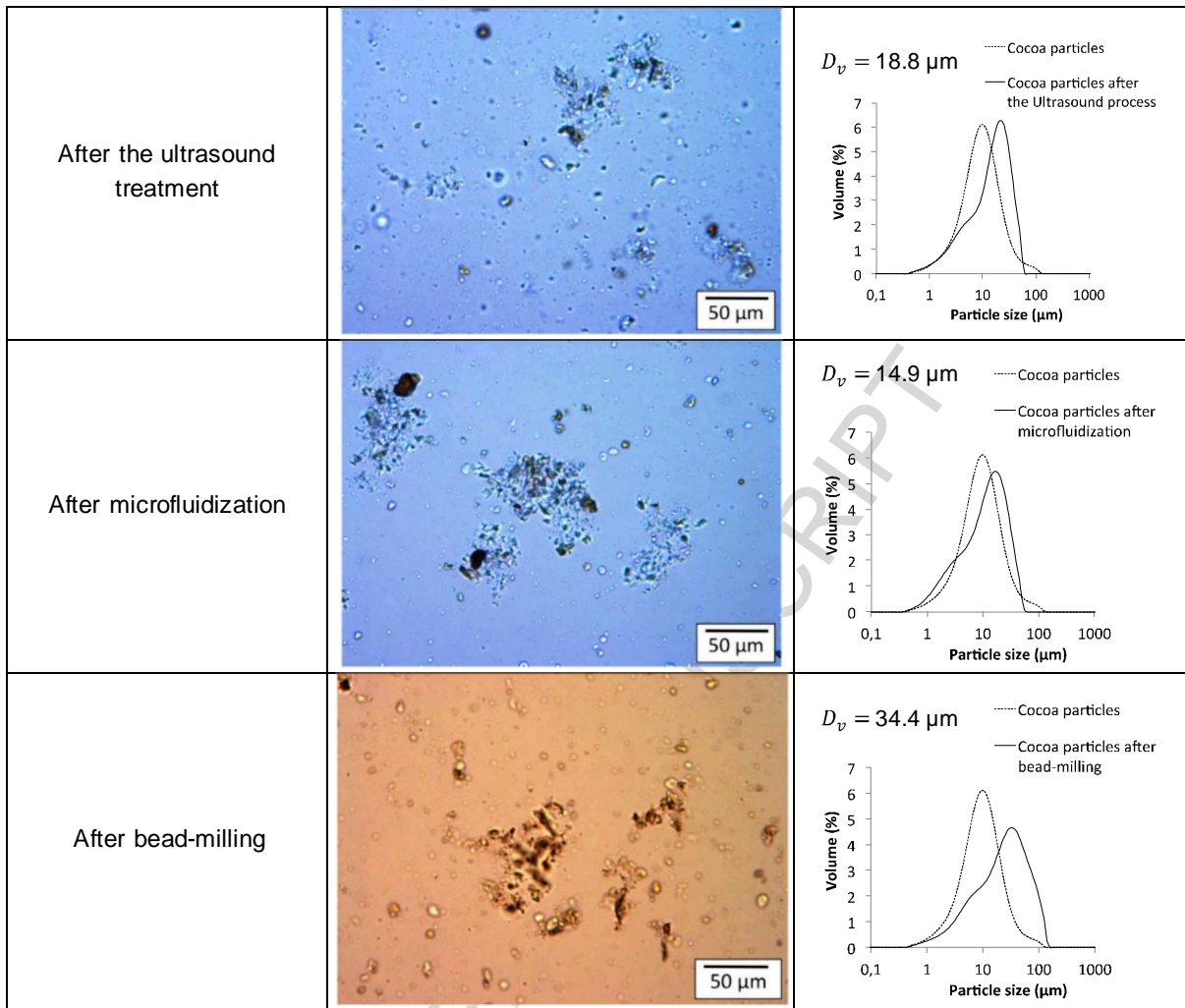


Figure 2

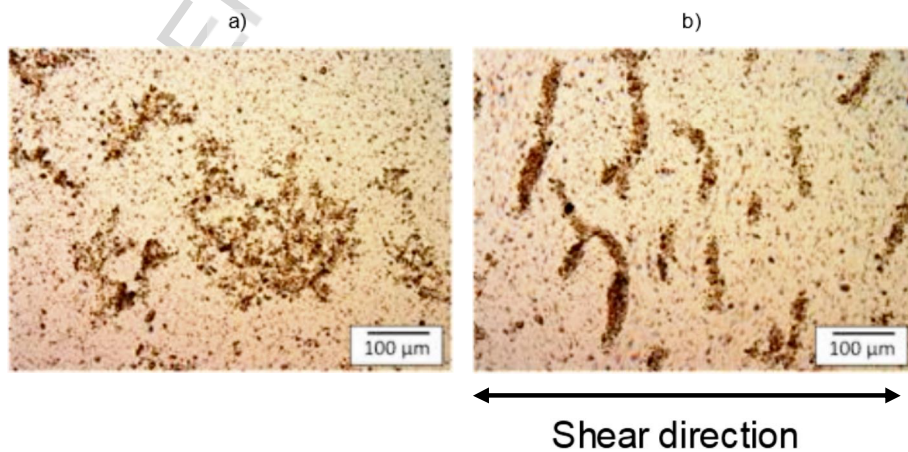


Figure 3

3.2. Influence of emulsification process on emulsions properties

Solid-stabilized emulsions were obtained using cocoa powder as sole emulsifier. In supplementary information (SI.3), we report microscope images of emulsions prepared with the Ultra-Turrax® mixer and ultra-sounds. Both adsorbed and non-adsorbed particles can be distinguished. A control emulsion was fabricated without cocoa powder. In this case, fast destabilization occurred with the formation of an oil layer at the top of the recipient after a few hours of settling. Instead, emulsions containing cocoa powder could be stored for at least several days without any apparent oil leakage. All these preliminary observations suggest that cocoa particles act as an emulsion stabilizer through a Pickering mechanism.

The impact of the emulsification process was studied on emulsions containing 20 wt.% oil and 2.5 wt.% cocoa powder with respect to the aqueous phase. The average diameters, polydispersities and anchoring ratios are given in Fig. 4. Data are in line with those reported in the previous section: the mixing conditions that produce particle unwrapping ensure better emulsification performances, *i.e.* smaller average droplet sizes, lower polydispersities and higher anchoring ratios. Microfluidization was the most efficient technique, followed by sonication and Ultra-Turrax® mixing. It can be argued that this ranking reflects the amplitude of the mixing energy densities. Compared with the two other techniques, microfluidization allows higher energy densities to be achieved (Sadeghpour Galooyak & Dabir, 2015; Slavka Tcholakova et al., 2011). As a consequence, solid particles are more efficiently unwrapped, which increases their surface area and their interfacial coverage capacity. Also, higher mixing intensities facilitate the attachment of particles to the oil-water interfaces since, during collisions, hydrodynamic forces push droplets towards particles' surfaces, which helps overcoming the energy barrier for adsorption.

Emulsification process	Anchoring ratio	D_v (μm)	P
Ultra-Turrax®	46%	11.6	0.73

Ultrasound	74%	9.5	0.59
Microfluidization	90%	4.2	0.38

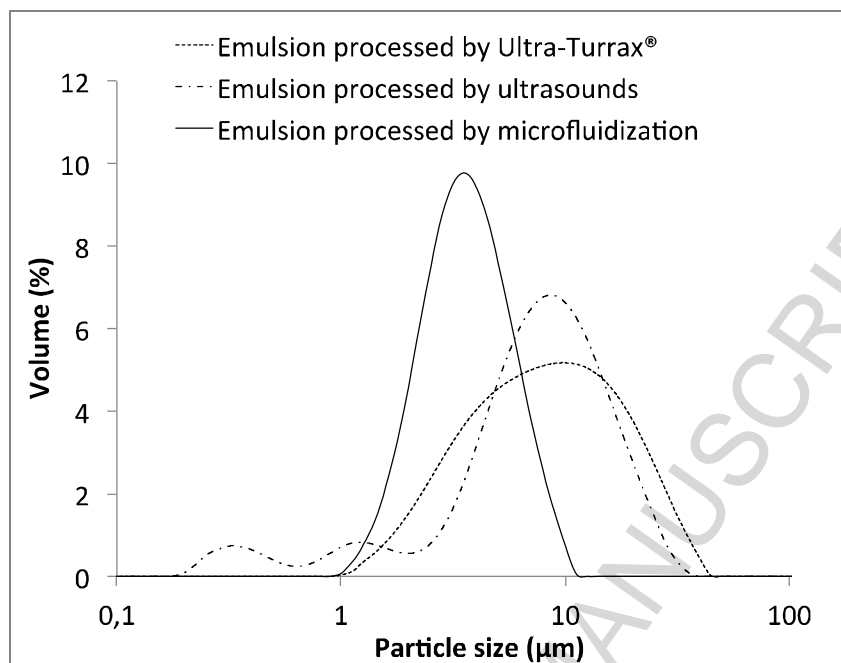


Figure 4

Irrespective of the emulsification technique, the average diameter of the particles was larger than 10 μm (Fig. 2) but oil droplets smaller than this characteristic size could be obtained (Fig. 4). This may seem surprising since the size of droplets is generally larger than that of the stabilizing particles in Pickering emulsions (Leal-Calderon & Schmitt, 2008). To clarify this issue, microscopic analysis of the emulsions was carried out under conventional white light (Fig. 5 column a) and under fluorescent conditions (Fig. 5 column b). The two adopted configurations are complementary, as phase contrast microscopy allows droplets visualization, whereas cocoa particles are revealed as bright red spots under fluorescent conditions. Figure 5 shows both types of microscopic images for the three emulsification processes. We would like to remind that free particles were removed from the continuous phase (see section 2.5) in order to better distinguish the interfaces.

Emulsions were always highly flocculated. Cocoa particles being relatively large (up to several tens of microns), they act as solid substrates likely to attach several oil droplets on their periphery. Do to their large size, they have a limited surface area for droplet adsorption. Such situation favor droplet bridging and the formation of large droplet flocs, as can be seen in Fig. 5. Droplets generated by sonication and microfluidization exhibit diffuse fluorescence in their whole surface reflecting the presence of thinner or smaller particles at the interface. Instead, fluorescence is localized as bright fluorescent isolated spots on the droplets surface for emulsions produced by Ultra-Turrax®, due to the presence of thicker cocoa particles.

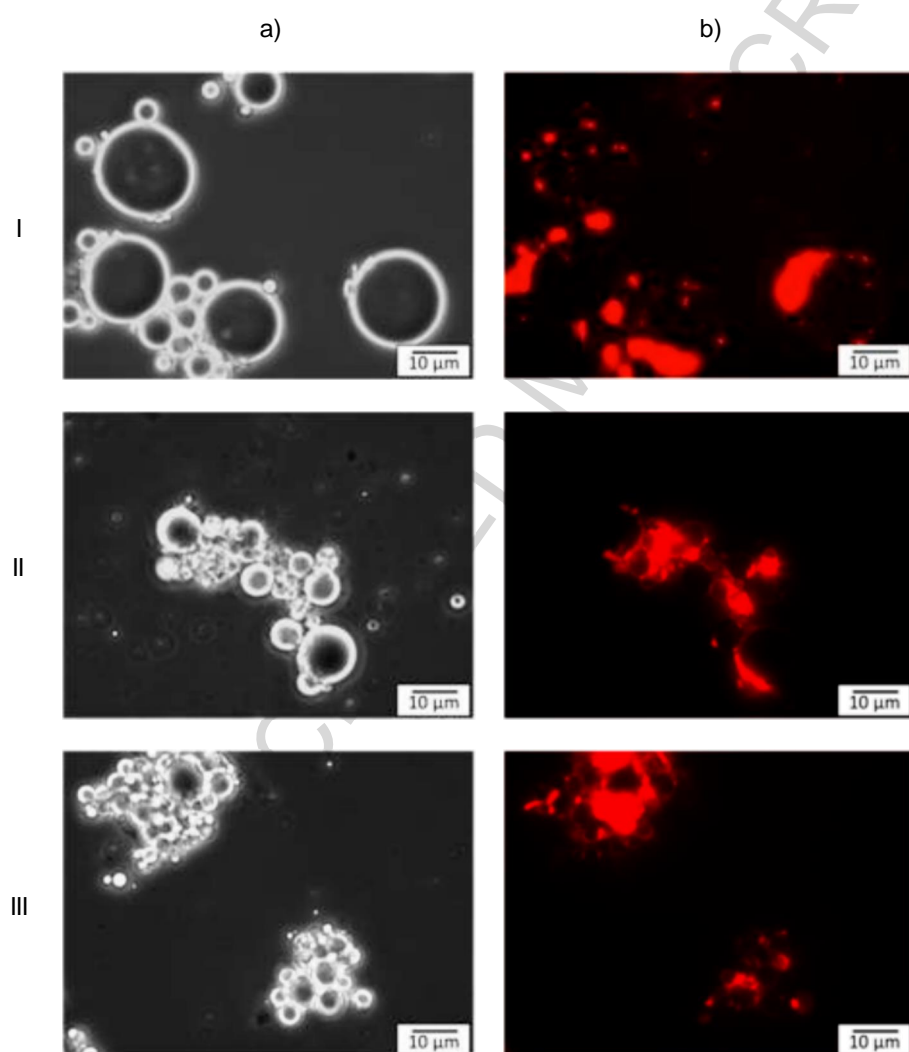


Figure 5

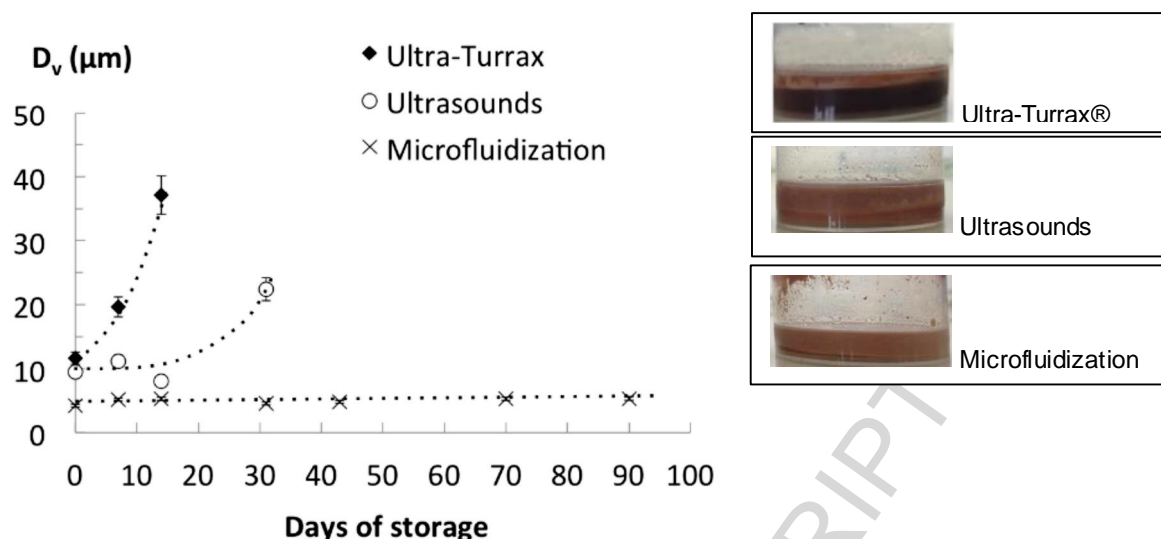


Figure 6

The kinetic stability of these emulsions was investigated by following their macroscopic aspect (creaming) and their average droplet size for 90 days (Fig. 6). Three layers were observed in all cases after a few days of storage: a cream, a dark intermediate phase almost devoid of droplets and a sediment containing free cocoa particles. Not surprisingly, we observed that the higher the anchoring ratio, the slower the creaming, the smaller the droplets and the better the stability. The emulsion obtained *via* microfluidization with the highest anchoring rate and the smallest droplets was indeed stable over at least 90 days with almost no evolution of its average droplet diameter, despite a slight creaming. This system was indeed highly viscous, with restricted dynamics, which precluded any significant structural evolution. Conversely, the average droplet size noticeably increased over time for the emulsion deriving from Ultra-Turrax® mixing. This emulsion was quite fluid and was prone to fast creaming. Size measurements were stopped after 14 days of storage, once an oil layer was observed at the top of the emulsion. The behavior of the emulsion deriving from sonication appeared to be intermediate between the two previous ones.

3.3. Influence of soluble compounds on emulsion stability

3.3.1. Quantification of soluble contents

Water-soluble compounds (proteins, carbohydrates, polyphenols) were titrated in a 10 wt.% dispersion of delipidated cocoa powder dispersed in deionized water, using the analytical techniques described in section 2.4. Soluble compounds were found to represent 23.6 ± 0.5 wt.% of the cocoa powder. The results concerning three classes of compounds are provided in Table 2. We would like to emphasize that the concentrations are expressed as equivalent concentrations of reference (calibration) molecules: glucose for carbohydrates, BSA for proteins and gallic acid for polyphenols (see section 2.4). The ash content of the powder was also measured and the obtained value was 10.5 wt.% of the initial delipidated cocoa mass, indicating that minerals were among the most abundant soluble compounds.

The soluble fraction was also measured and analyzed in the cocoa dispersion processed in the microfluidizer, and in the aqueous phase of emulsions with the same composition (10 wt.% of cocoa powder in the aqueous phase, 20 wt.% oil), deriving from two emulsification techniques, right after their preparation. The results are also reported in Table 2. The soluble fraction remaining in the continuous phase for the emulsion obtained *via* microfluidization (19.5 wt.%) was slightly lower than in the other cases (~23 wt.%), probably because of the adsorption of proteins, the formation of insoluble protein/polyphenol complexes or the solubilization of some species in the oil phase (Foegeding, Plundrich, Schneider, Campbell, & Lila, 2017).

Table 2: Soluble fraction of cocoa powder dispersion processed in the microfluidizer and in the aqueous phase of emulsions with the same composition (10 wt.% of cocoa powder in the aqueous phase, 20 wt.% oil), obtained with 2 emulsification techniques. Data relative to the cocoa dispersion alone (no oil) are given as a reference. The contents are expressed as weight percentages of the initial cocoa mass present in the aqueous phase. The values are means of 3 measurements.

Total soluble fraction	Carbohydrates (eq. Glucose)	Proteins (eq. BSA)	Polyphenols (eq. Gallic)
------------------------	-----------------------------	--------------------	--------------------------

	acid)			
Cocoa dispersion alone (10 wt%)	23.6 ± 0.1 %	6.6 ± 0.3 %	1.36 ± 0.05 %	1.21 ± 0.04 %
Cocoa dispersion processed in the microfluidizer (800 bars)	22.0 ± 0.3 %	6.4 ± 0.3 %	1.53 ± 0.30 %	1.26 ± 0.20 %
Emulsion obtained by Ultra-Turrax®	25.9 ± 0.8 %	6.3 ± 0.3 %	1.12 ± 0.06 %	0.88 ± 0.09 %
Emulsion obtained by Microfluidization (800 bars)	19.5 ± 1.4 %	6.3 ± 0.4 %	0.61 ± 0.03 %	0.72 ± 0.07 %

3.3.2. Comparison of emulsions with and without soluble fraction

Since some of the soluble compounds like proteins, are known to have surface-activity, they can potentially contribute to emulsion stabilization. To assess the potential role of soluble compounds regarding emulsification and kinetic stabilization, emulsions containing 20 wt.% oil were fabricated with the microfluidizer at 800 bars, using three delipidated powder fractions deriving from the same source: (1) the whole cocoa powder, (2) the cocoa powder without soluble compounds, containing only particles, and (3) the soluble fraction only. Emulsion (1) contained 2.5 wt.% of the whole cocoa powder with respect to the aqueous phase. In order to make a meaningful comparison, the amount of powder in emulsion (2) was fixed to introduce approximately the same amount of (insoluble) particles as in emulsion (1), namely 2 wt.%. In the same way, emulsion (3) contained approximately the same amount of soluble compounds as emulsion (1), *i.e.* 0.5 wt.%. It is worth noting that the powder without soluble compounds was processed twice in the microfluidizer, once for the extraction of the soluble compounds (see section 2.4) and once for the emulsification process. To keep the same operating conditions, the dispersion of whole cocoa powder was primarily processed in the microfluidizer at 800 bars prior to the emulsification. In Fig. 7, we report the kinetic evolution of the average droplet size for the three emulsions. The emulsion without soluble compounds had exactly the same features as the one obtained with the original whole cocoa powder in terms of initial droplet size and stability. The anchoring ratios were also quite similar for both emulsions, close to 90%. It can thus be concluded that the soluble fraction as part of the whole cocoa powder has no impact on the emulsification

process and on the stability. Yet, this fraction, when used alone, displayed some functionality as an emulsion could be obtained upon microfluidization. However, this emulsion was initially quite coarse and underwent a significant increase of its average droplet size over time, as can be observed in Fig. 7.

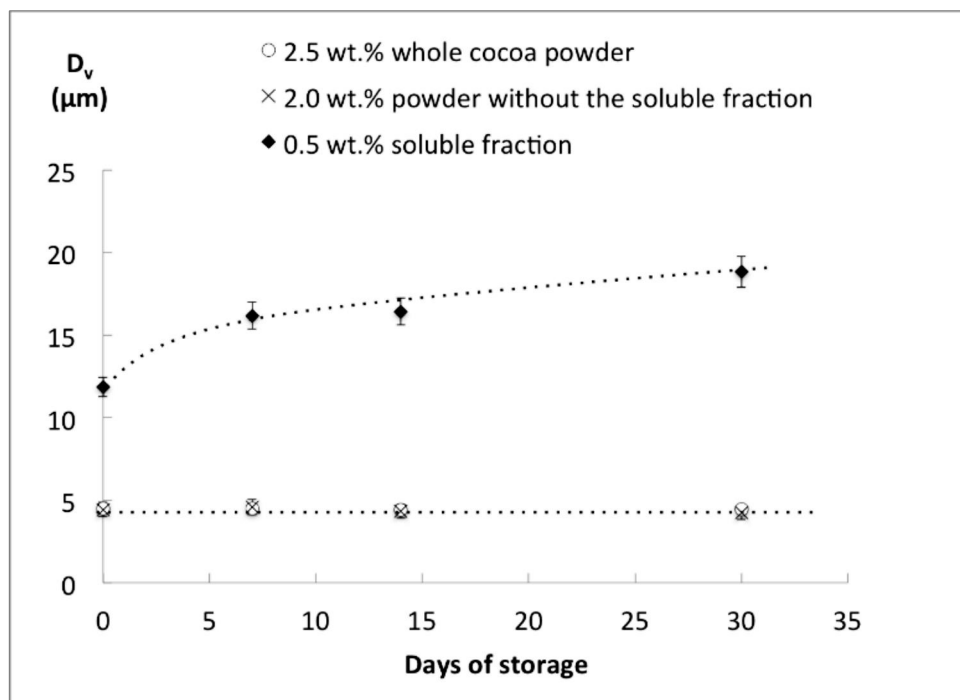


Figure 7

3.4. Influence of the fraction of fine particles

A dispersion containing 10 wt.% cocoa powder in deionized water was submitted to microfluidization at 800 bars and was then diluted at 2.5 wt.%. This dispersion was allowed to sediment for 24h. The supernatant containing fine (Brownian) particles and soluble compounds was removed. These two components were separated following the method described in section 2.4. As mentioned in section 3.1, fine particles were found to represent around 10 wt.% of the total mass of cocoa powder and they had an average size deduced from DLS of 1.35 μm. For the sake of comparison, we also analyzed the fraction of fine particles in an unprocessed powder. The fraction was found to be 8.9 wt.% and the average particle size was 1.64 μm. It can be concluded that the mechanical treatment imposed during the emulsification process does not significantly modify the amount of fine particles.

To evaluate the impact of fine particles on both emulsification and stabilization, we compared three emulsions fabricated by microfluidization at 800 bars with the following powder fractions in the aqueous phase: (1) whole cocoa powder at 2.5 wt.%, (2) powder with only coarse particles at 1.75wt.% (=0.7×2.5wt.%), and (3) powder with only the fine fraction at 0.25wt.% (=0.1×2.5wt.%). In the two latter systems, the powder content in the aqueous phase was selected so as to introduce approximately the same amount of the components (large particles in system (2) and fine particles in system (3)) as in the system based on whole cocoa powder (1) (~20 wt.% soluble compounds, 10 wt.% fine Brownian particles and 70 wt.% coarse particles). Micrographs of the corresponding emulsions under conventional white light illumination and fluorescent configuration are provided in Supplementary Information SI.4. The kinetic evolution of the average droplet sizes are reported in Fig. 8. The similarity in the behavior of systems (1) and (2) leads to the conclusion that fine particles have a negligible influence on emulsion stabilization.

At 0.25 wt.%, the emulsion formulated with fine particles only has a very large average diameter, around 45 μm . To further probe the functionality of this fraction, the content was increased up to 2.5 wt.%. In this case, we obtained an emulsion with $D_v = 7 \mu\text{m}$, $P = 0.37$, and an anchoring ratio of $90 \pm 5 \%$ (See supplementary information, SI.5). Its diameter did not evolve after 30 days of storage. It can thus be stated that fine particles do not have a noticeable influence, as they are masked by the major fraction of cocoa powder made of large particles. However, they do have *per se* the ability to stabilize emulsions at sufficiently large concentrations.

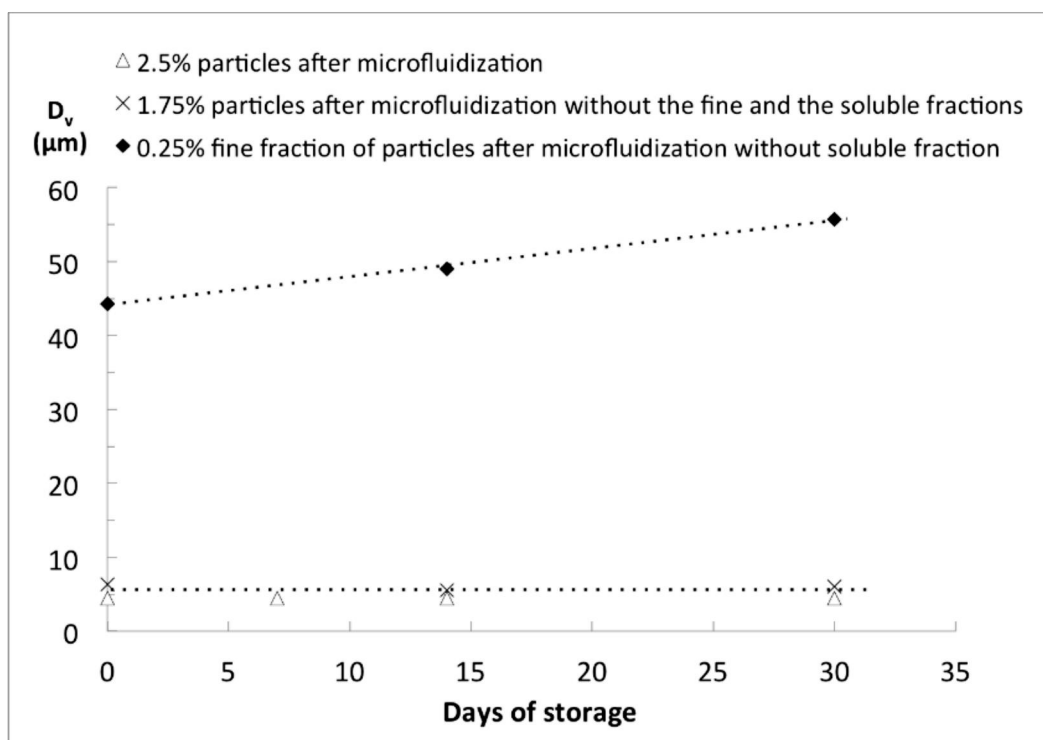


Figure 8

3.5. Influence of the homogenization pressure

Since microfluidization led to the best performances, a specific study was carried out using this technique. We first examined the influence of the applied pressure by comparing the same formulation (2.5 wt.% cocoa powder in the aqueous phase and 20 wt.% sunflower oil) emulsified at 240, 500 and 800 bars. In all cases, the number of passes in the homogenizing chamber was fixed to 6. Microscopic observations as well as emulsion specifications are gathered in Fig. 9. It clearly appears that the average droplet size and polydispersity decrease with the homogenizing pressure. Droplets are bigger at low pressure despite they have comparable anchoring ratios.

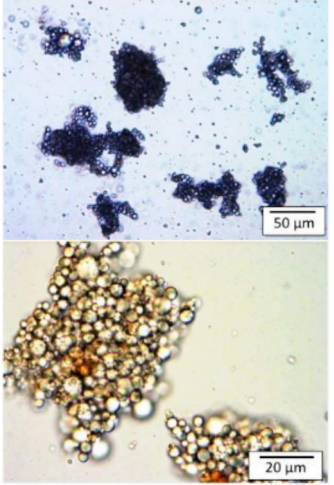
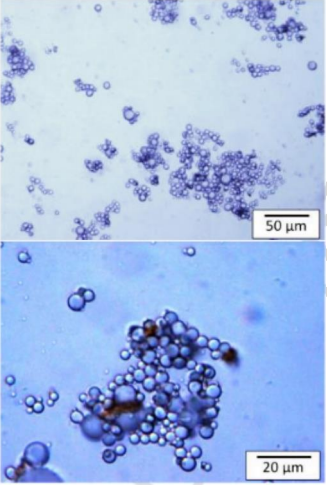
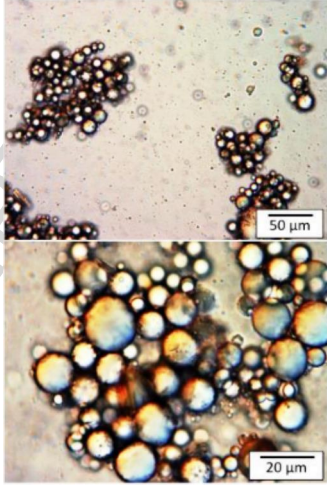
Pressure	800 bars (a)	500 bars (b)	240 bars (c)
Microscopy			
Dv / P	4.2 µm / 0.38	5.9 µm / 0.46	10.9 µm / 0.54
Anchoring ratio	90 ± 5%	90 ± 5%	95 ± 5%

Figure 9

The high anchoring ratios explain why emulsions remained kinetically stable over a 90-day period (Fig. 10): droplets are well covered and entangled in the particles network, impeding coalescence. The difference in droplet size can be explained by a difference in surface activity. Considering the results of section 3.1, it can be argued that the surface-active moieties and/or components in the powder become increasingly accessible as the homogenizing pressure increases, due to particle unwrapping.

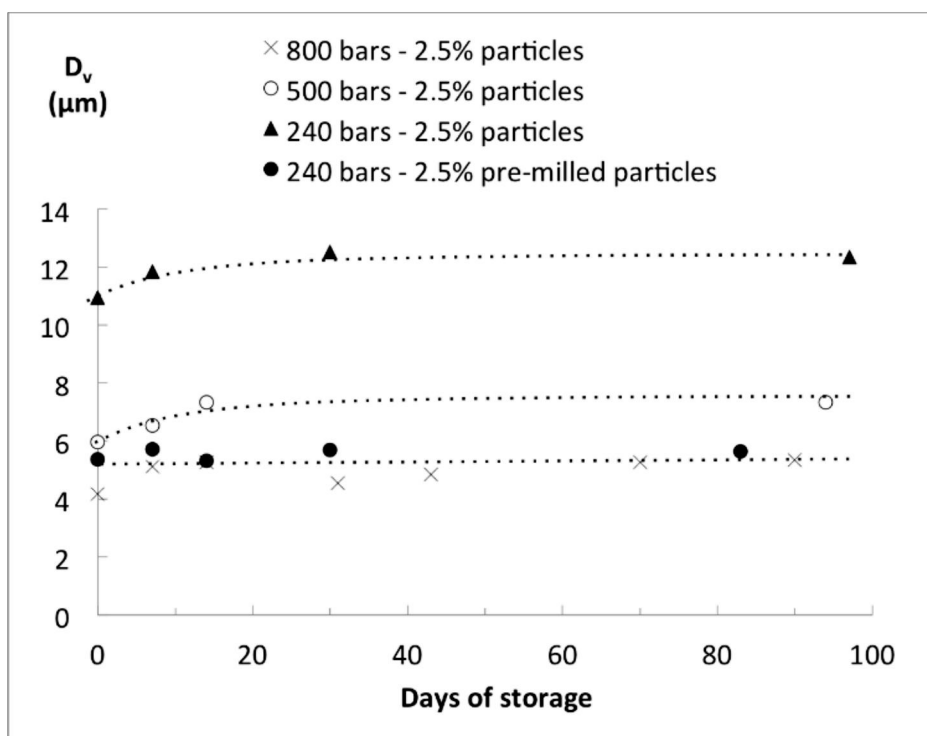


Figure 10

3.6. Impact of particles pre-milling

In practical applications, it may be interesting to make use of pre-processed particles, whose unwrapping extent is sufficient to carry on emulsification at low homogenizing pressures. We thus studied the impact of a preliminary bead-milling step of the cocoa powder, as this technique is known to efficiently refine and disperse a wide variety of solid matters.

The evolution of the average droplet size of an emulsion obtained by microfluidization at 240 bars and prepared from pre-milled particles (see section 2.2) is also shown in Fig. 10. The micrographs of the corresponding emulsion are provided in Fig. 11.

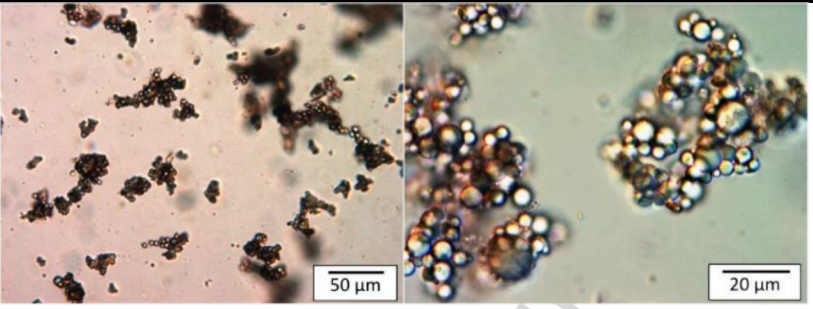
Conditions	240 bar with pre-milling	
Microscopy		
D_v / P	5.4 µm / 0.41	
Anchoring ratio	90 ± 5%	

Figure 11

In all cases, the anchoring ratio was close to 90%. The properties of emulsions fabricated at 240 bars with pre-milled particles are comparable to those of the emulsion obtained at 800 bars without pre-milling. By comparison, the emulsion generated at 240 bars with unprocessed particles has a significantly higher average diameter (10.9 µm vs. 5.4 µm). It can thus be concluded that the pre-milling step has an added value, as it allows decreasing the homogenizing pressure during the emulsification step. Again, it can be argued that milling reveals more surface-active “anchoring sites” (Tamayo Tenorio, Gieteling, Nikiforidis, Boom, & van der Goot, 2017; Wallecan, McCrae, Debon, Dong, & Mazoyer, 2015) or equivalently increases their specific surface area, which enhances their adsorption capacity at the oil/water interface. The more numerous the anchoring sites, the smaller the average droplet size.

3.7. Influence of particle amount on droplet size

In general, solid particles are irreversibly anchored at an oil-water interface (Berton-Carabin & Schroën, 2015; Rayner et al., 2014; Wiley, 1954). If the amount of particles is insufficient to fully cover the interfacial area generated by the homogeneization process, the

fragmented drops recombine until the level of interfacial coverage becomes sufficient to ensure stability (limited coalescence), giving rise to droplets with a very narrow size distribution. We used microfluidization at 800 bars, which is a high energy emulsification process. Because of the very high applied shear rates, it is expected that smaller drops, as compared to those in the final emulsions (their diameter always exceeded 2,7 μm in our study), are initially formed in the processing volume of the microfluidizer. As a result, recoalescence of the drops must take place within and after the processing element, so that larger drops are formed in the final emulsion. In this concentration range, the final surface-averaged diameter, D_s , is expected to follow the relation (Arditty et al., 2003):

$$S = \frac{6V}{D_s} = s_f m_a \quad (4)$$

where V (m^3) is the volume of the dispersed phase, m_a (g) is the mass of adsorbed particles for the total emulsion, and s_f ($\text{m}^2 \cdot \text{g}^{-1}$) is the specific surface area, *i.e.* the area that can be stabilized by 1g of particles. This parameter can be determined from the slope of the curve representing the evolution of the total surface area of the droplets, S , as a function of m_a , at constant volume of the oil phase. Thus, in the limited coalescence regime, the mean droplet size after emulsification is only governed by a critical value of the surface coverage, s_f , and is not supposed to depend on the hydrodynamic conditions (Tcholakova et al., 2002). This was verified in our case since the average droplet size obtained with pre-milled particles at 2.5 wt.% in the aqueous phase was the same at 240 and 800 bars.

The mass of cocoa powder was varied from 0.15g to 2.5g (from around 1 wt.% to 15 wt.% of the aqueous phase) in emulsions containing 10, 20 and 30 wt.% oil. The homogenizing pressure was set at 800 bars. We deduced the total surface area of the droplets from their surface-averaged diameter, D_s , measured by light scattering, and the mass of adsorbed particles from the anchoring ratio:

$$m_a = \frac{(\text{anchoring ratio} \times m_p^i)}{100} \approx \frac{(\text{anchoring ratio} \times 0.8 \times m_p)}{100} \quad (5)$$

The anchoring ratio was measured for each experimental point and was found to be close to 90%. In Fig. 12, we plot the variation of S , measured right after emulsion fabrication, as a function of the mass of adsorbed particles, m_a , at constant V . The curves display a linear regime with a pronounced slope, and a non-linear regime in which S is weakly varying with m_a , whatever the oil content. At small powder content, the linearity of the plot gives a hint that the final size is determined by the limited coalescence process. The specific surface area of the particles, s_f , deduced from the slope is $\sim 16 \text{ m}^2\cdot\text{g}^{-1}$. This value is in the same order of magnitude as the one found by Wallecan et al. (2015) in emulsions stabilized by citrus fibers prepared by high pressure homogenization at 420 bars: $3 \text{ m}^2\cdot\text{g}^{-1}$. For the sake of comparison, the s_f value for proteins is of the order of several thousand $\text{m}^2\cdot\text{g}^{-1}$ (Dimitrova, Leal-Calderon, Gurkov, & Campbell, 2004; Slavka Tcholakova, Denkov, Ivanov, & Campbell, 2002), reflecting the much smaller size of proteins and consequently the much higher amount of available sites for adsorption, per unit mass of stabilizing material.

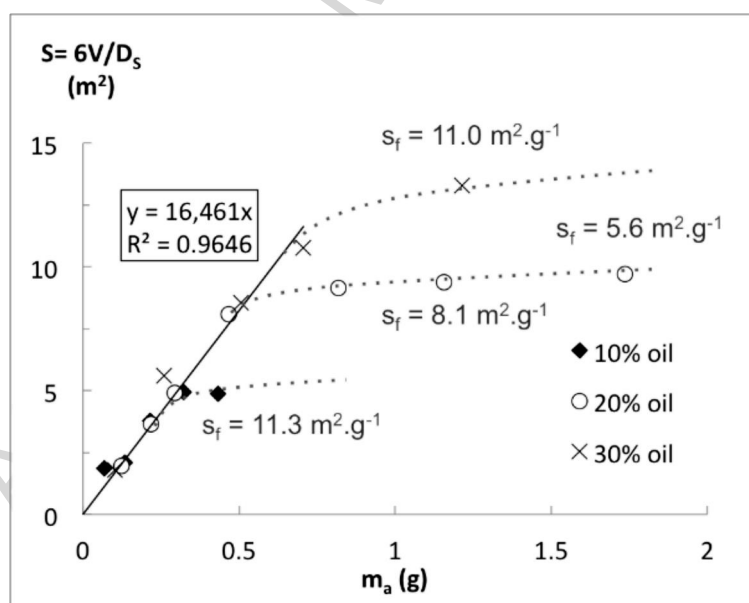


Figure 12

Above some critical particle content, which depends on the oil fraction, there is a clear deviation from the linear behavior. In this regime, the emulsification process becomes less

efficient as the total surface area of the droplets hardly varies and the anchoring ratio falls below 80%. The specific surface area also tends to regularly decrease (for each oil content, the value corresponding to the highest powder concentrations is indicated on the graph). The viscosity of the aqueous phase raised with the powder content and a strong gel was formed at the highest contents. It is likely that particle aggregation limits the availability of the anchoring sites (masking effect). The systems can be seen as gels made of interconnected particles with embedded droplets. In Fig. 12, we observe that the extent of the linear domain increases with the oil fraction. It can be argued that a larger amount of oil mobilizes more particles at the interfaces and consequently the “masking effect” due to bulk aggregates appears at higher particle concentrations.

3.8. Influence of oil content on droplet size

The oil content was varied from 10 to 50 wt.%, while maintaining the total mass of powder constant (1.5 wt.% with respect to the total mass of emulsion). The emulsification was performed by microfluidization at 800 bars. In Fig. 13, we plotted the product $D_s m_a$ (D_s was measured right after fabrication) as a function of V .

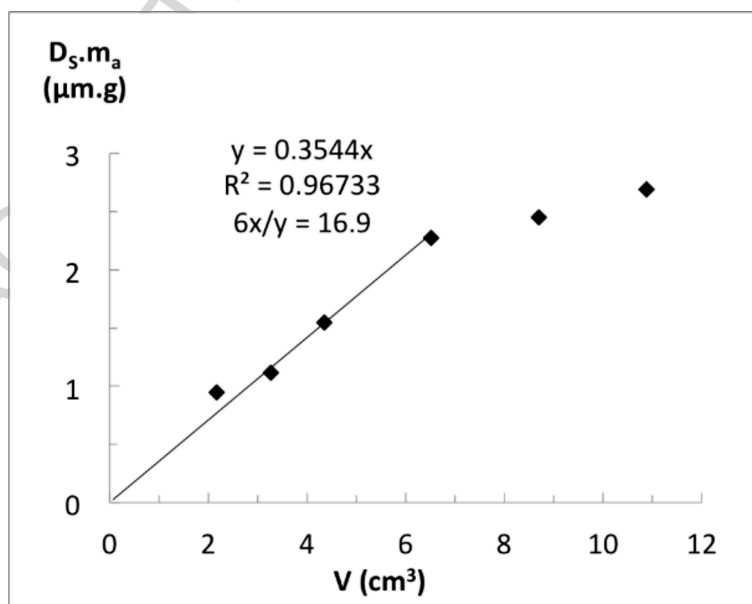


Figure 13

For low V values, Eq. (4) predicts a linear dependence with a slope equal to $6/s_f$. A value of s_f close to $17 \text{ m}^2.\text{g}^{-1}$ is obtained from the slope, in good agreement with that deduced from the linear regime in Fig. 12. At higher V values, the curve deviates from linearity, with a local slope tending to decrease (equivalently, s_f increases). As the oil concentration increases, the inter-droplet distance decreases, which favors the formation of particulate bridges between the drops and thus emulsion gelation. In our case, although the rheological properties were not measured, we observed that the systems with the highest oil fractions resembled to viscoelastic pastes, whereas those obtained at the lowest oil contents remained comparatively more fluid and underwent short-time creaming (see supplementary information, SI.6). As the connectivity increases, the internal dynamics in the emulsion gel are considerably slowed down. As a result of such mobility hindering, limited coalescence would be interrupted at earlier stages, thus generating emulsions whose effective s_f value is higher than in the linear regime, at the origin of the deviation observed in Fig. 13.

Conclusion

This paper was concerned with the impact of the emulsification process and of some formulations parameters on the properties of oil-in-water Pickering emulsions stabilized by cocoa particles. We developed protocols to reliably measure the fraction of particles adsorbed at the oil/water interface and the droplet size distribution. Emulsion stabilization was described as being due to surface-active moieties present in the particles, and stabilization due to physical trapping of droplets in the particles network. Among the three emulsification techniques that were probed, microfluidization was the most efficient one, as it allowed obtaining the finest emulsions and the highest anchoring ratios. This highly energetic process is likely to increase the number of available surface-active moieties by unwrapping cocoa particles that act as droplets collectors. A rise in the pressure imposed during

microfluidization as well as a pre-milling of the particles were shown to improve emulsions performances. Soluble compounds and fine particles ($< \text{c.a. } 2 \mu\text{m}$) were shown to have a negligible impact in emulsification. Despite the intrinsic chemical and physical complexity of cocoa particles which are both polydisperse in size and shape, emulsions with narrow droplet size distributions could be obtained. In the particle-poor regime, the evolution of the average size obeyed a simple law characterized by a unique coverage parameter independent of the total oil amount.

The methodology developed here can be utilized to study other emulsions based on particles of vegetable origin. Stabilization by other plant materials are under current investigation.

Acknowledgements

This work was performed, in partnership with the SAS PIVERT, within the frame of the French Institute for the Energy Transition (Institut pour la Transition Energétique (ITE)) P.I.V.E.R.T (www.institut-pivert.com) selected as an investment for the Future (« Investissement d'Avenir »). This work was supported, as a part of the Investments for the Future, by the French Government under the reference ANR-001-01.

Figure captions

Figure 1: Microscopic observations at two magnification levels of an emulsion composed of 4 wt.% cocoa powder and 20 wt.% sunflower oil, fabricated by microfluidization at 800 bars before and after SDS treatment.

Figure 2: Microscopic observations and size data of cocoa particles after mechanical processing.

Figure 3: Windings formed by large cocoa particles in the direction perpendicular to the applied shear (indicated by the arrows): before (a) and after (b) shearing.

Figure 4: Initial anchoring ratios, volume-averaged diameter, polydispersity and size distributions of emulsions prepared with 2.5 wt.% cocoa powder.

Figure 5: Phase contrast microscopic (a), and fluorescence microscopic (b) images of different emulsions processed by Ultra-Turrax® (I), ultrasounds (II), and microfluidization (III).

Figure 6: Evolution of the average droplet diameter for emulsions (2.5wt.% cocoa powder) obtained by different emulsification processes and macroscopic aspect of the corresponding emulsions after 45 days. Dotted lines are guides for the eyes.

Figure 7: Kinetic evolution of the average droplet size of emulsions containing 20 wt.% oil, fabricated with the microfluidizer at 800 bars, using three delipidated powder fractions deriving from the same source. Dotted lines are guides for the eyes.

Figure 8: Evolution of the average droplet diameter for emulsions containing 20 wt.% oil, obtained with different fractions of the cocoa powder. Dotted lines are guides for the eyes.

Figure 9: Microscopic observations and main characteristics of emulsions containing 2.5 wt.% of cocoa powder in the aqueous phase and 20 wt.% oil, prepared by microfluidization at different pressures.

Figure 10: Evolution of the droplet average diameter for emulsions containing 2.5 wt.% of cocoa powder in the aqueous phase and 20 wt.% oil, obtained by microfluidization at different pressures. For 240 bars, the cocoa particles were pre-milled or not. Dotted lines are guides for the eyes.

Figure 11: Microscopic images of the emulsions containing 2.5 wt.% of cocoa powder in the aqueous phase and 20 wt.% oil, obtained by microfluidization at 240 bars with a pre-milling step.

Figure 12: Total surface area as a function of the mass of adsorbed particles for three oil contents. The total mass of emulsion is 20 g.

Figure 13: Influence of the oil content on the product $D_s m_a$, where D_s is the surface-averaged diameter of the emulsion droplets right after fabrication and m_a is the mass of adsorbed particles. The total mass of emulsion is 20 g.

References

- Arditty, S., Whitby, C. P., Binks, B. P., Schmitt, V., & Leal-Calderon, F. (2003). Some general features of limited coalescence in solid-stabilized emulsions. *The European Physical Journal E*, 11(3), 273–281. <https://doi.org/10.1140/epje/i2003-10018-6>
- Ashby, N. P., & Binks, B. P. (2000). Pickering emulsions stabilised by Laponite clay particles. *Physical Chemistry Chemical Physics*, 2(24), 5640–5646. <https://doi.org/10.1039/B007098J>
- Berne, B. J., & Pecora, R. (1976). *Dynamic light scattering: with applications to chemistry, biology, and physics*. Courier Corporation.
- Berton-Carabin, C. C., & Schroën, K. (2015). Pickering Emulsions for Food Applications: Background, Trends, and Challenges. *Annual Review of Food Science and Technology*, 6(1), 263–297. <https://doi.org/10.1146/annurev-food-081114-110822>
- Binks, B. P. (2002). Particles as surfactants—similarities and differences. *Current Opinion in Colloid & Interface Science*, 7(1), 21–41. [https://doi.org/http://dx.doi.org/10.1016/S1359-0294\(02\)00008-0](https://doi.org/http://dx.doi.org/10.1016/S1359-0294(02)00008-0)
- Binks, B. P. (2017). Colloidal Particles at a Range of Fluid–Fluid Interfaces. *Langmuir*. <https://doi.org/10.1021/acs.langmuir.7b00860>
- Binks, B. P., & Lumsdon, S. O. (2001). Pickering Emulsions Stabilized by Monodisperse Latex Particles: Effects of Particle Size. *Langmuir*, 17(15), 4540–4547. <https://doi.org/10.1021/la0103822>
- Campbell, A. L., Holt, B. L., Stoyanov, S. D., & Paunov, V. N. (2008). Scalable fabrication of anisotropic micro-rods from food-grade materials using an in shear flow dispersion-solvent attrition technique. *J. Mater. Chem.*, 18(34), 4074–4078.

<https://doi.org/10.1039/B807738J>

Destribats, M., Rouvet, M., Gehin-Delval, C., Schmitt, C., & Binks, B. P. (2014). Emulsions stabilised by whey protein microgel particles: towards food-grade Pickering emulsions. *Soft Matter*, *10*(36), 6941–6954.

<https://doi.org/10.1039/C4SM00179F>

Dimitrova, T. D., Leal-Calderon, F., Gurkov, T. D., & Campbell, B. (2004). Surface forces in model oil-in-water emulsions stabilized by proteins. *Advances in Colloid and Interface Science*, *108-109*, 73—86. <https://doi.org/10.1016/j.cis.2003.10.003>

Finkle, P., Draper, H. D., & Hildebrand, J. H. (1923). The theory of emulsification. *Journal of the American Chemical Society*, *45*(12), 2780–2788.

<https://doi.org/10.1021/ja01665a002>

Foegeding, E. A., Plundrich, N., Schneider, M., Campbell, C., & Lila, M. A. (2017). Protein-polyphenol particles for delivering structural and health functionality. *Food Hydrocolloids*, *72*, 163–173. <https://doi.org/10.1016/j.foodhyd.2017.05.024>

Golemanov, K., Tcholakova, S., Kralchevsky, P. A., Ananthapadmanabhan, K. P., & Lips, A. (2006). Latex-Particle-Stabilized Emulsions of Anti-Bancroft Type. *Langmuir*, *22*(11), 4968–4977. <https://doi.org/10.1021/la0603875>

Gould, J., Vieira, J., & Wolf, B. (2013). Cocoa particles for food emulsion stabilisation. *Food & Function*, *4*(9), 1369–1375.

<https://doi.org/10.1039/C3FO30181H>

Leal-Calderon, F., & Schmitt, V. (2008). Solid-stabilized emulsions. *Current Opinion in Colloid & Interface Science*, *13*(4), 217–227.

<https://doi.org/10.1016/j.cocis.2007.09.005>

Leclercq, L., Mouret, A., Proust, A., Schmitt, V., Bauduin, P., Aubry, J.-M., & Nardello-Rataj, V. (2012). Pickering Emulsion Stabilized by Catalytic

Polyoxometalate Nanoparticles: A New Effective Medium for Oxidation Reactions. *Chemistry - A European Journal*, 18(45), 14352–14358.

<https://doi.org/10.1002/chem.201201799>

Lecumberri, E., Mateos, R., Izquierdo-Pulido, M., Rupérez, P., Goya, L., & Bravo, L. (2007). Dietary fibre composition, antioxidant capacity and physico-chemical properties of a fibre-rich product from cocoa (*Theobroma cacao* L.). *Food Chemistry*, 104(3), 948–954. <https://doi.org/10.1016/j.foodchem.2006.12.054>

Leyva, A., Quintana, A., Sánchez, M., Rodríguez, E. N., Cremata, J., & Sánchez, J. C. (2008). Rapid and sensitive anthrone-sulfuric acid assay in microplate format to quantify carbohydrate in biopharmaceutical products: method development and validation. *Biologicals: Journal of the International Association of Biological Standardization*, 36(2), 134–141. <https://doi.org/10.1016/j.biologicals.2007.09.001>

Luo, Z., Murray, B. S., Yusoff, A., Morgan, M. R. A., Povey, M. J. W., & Day, A. J. (2011). Particle-Stabilizing Effects of Flavonoids at the Oil–Water Interface. *Journal of Agricultural and Food Chemistry*, 59(6), 2636–2645. <https://doi.org/10.1021/jf1041855>

Mackie, A. R., Gunning, A. P., Wilde, P. J., & Morris, V. J. (2000). Competitive displacement of β -lactoglobulin from the air/water interface by sodium dodecyl sulfate. *Langmuir*, 16(21), 8176–8181.

Noble, J. E., & Bailey, M. J. A. (2009). Quantitation of Protein Chapter 8. In R. R. Burgess & M. P. Deutscher (Eds.), *Guide to Protein Purification, 2nd Edition* (Vol. 463, pp. 73–95). Academic Press. Retrieved from <http://www.sciencedirect.com/science/article/pii/S0076687909630081>

Pickering, S. U. (1907). CXCVI.—Emulsions. *Journal of the Chemical Society, Transactions*, 91(0), 2001–2021. <https://doi.org/10.1039/CT9079102001>

Pradines, V., Krägel, J., Fainerman, V. B., & Miller, R. (2008). Interfacial properties of mixed β -lactoglobulin- SDS layers at the water/air and water/oil interface. *The Journal of Physical Chemistry B*, 113(3), 745–751.

Ramsden, W. (1903). Separation of Solids in the Surface-Layers of Solutions and “Suspensions” (Observations on Surface-Membranes, Bubbles, Emulsions, and Mechanical Coagulation). -- Preliminary Account. *Proceedings of the Royal Society of London*, 72(477-486), 156–164. <https://doi.org/10.1098/rspl.1903.0034>

Rayner, M., Marku, D., Eriksson, M., Sjöo, M., Dejmek, P., & Wahlgren, M. (2014). Biomass-based particles for the formulation of Pickering type emulsions in food and topical applications. *Colloids and Surfaces A: Physicochemical and Engineering Aspects*, 458, 48–62. <https://doi.org/10.1016/j.colsurfa.2014.03.053>

Sadeghpour Galooyak, S., & Dabir, B. (2015). Three-factor response surface optimization of nano-emulsion formation using a microfluidizer. *Journal of Food Science and Technology*, 52(5), 2558–2571. <https://doi.org/10.1007/s13197-014-1363-1>

Sarkar, A., Li, H., Cray, D., & Boxall, S. (2018). Composite whey protein–cellulose nanocrystals at oil-water interface: Towards delaying lipid digestion. *Food Hydrocolloids*, 77, 436–444. <https://doi.org/10.1016/j.foodhyd.2017.10.020>

Sarkar, A., Murray, B., Holmes, M., Ettelaie, R., Abdalla, A., & Yang, X. (2016). In vitro digestion of Pickering emulsions stabilized by soft whey protein microgel particles: influence of thermal treatment. *Soft Matter*, 12(15), 3558–3569.

Sarkar, A., Zhang, S., Murray, B., Russell, J. A., & Boxal, S. (2017). Modulating in vitro gastric digestion of emulsions using composite whey protein-cellulose nanocrystal interfaces. *Colloids and Surfaces B: Biointerfaces*, 158, 137–146.

<https://doi.org/https://doi.org/10.1016/j.colsurfb.2017.06.037>

Shao, Y., & Tang, C.-H. (2016). Gel-like pea protein Pickering emulsions at pH 3.0 as a potential intestine-targeted and sustained-release delivery system for β -carotene. *Food Research International*, *79*, 64–72.

Tamayo Tenorio, A., Gieteling, J., Nikiforidis, C. V., Boom, R. M., & van der Goot, A. J. (2017). Interfacial properties of green leaf cellulosic particles. *Food Hydrocolloids*, *71*, 8–16. <https://doi.org/10.1016/j.foodhyd.2017.04.030>

Tcholakova, S.; Denkov, N. D.; Ivanov, I. B.; Campbell, B. Coalescence in β -Lactoglobulin-Stabilized Emulsions: Effects of Protein Adsorption and Drop Size. *Langmuir* **2002**, *18* (23), 8960–8971

Tcholakova, S., D. Denkov, N., & Lips, A. (2008). Comparison of solid particles, globular proteins and surfactants as emulsifiers. *Physical Chemistry Chemical Physics*, *10*(12), 1608–1627. <https://doi.org/10.1039/B715933C>

Tcholakova, S., Denkov, N. D., Ivanov, I. B., & Campbell, B. (2002). Coalescence in β -Lactoglobulin-Stabilized Emulsions: Effects of Protein Adsorption and Drop Size. *Langmuir*, *18*(23), 8960–8971. <https://doi.org/10.1021/la0258188>

Tcholakova, S., Lesov, I., Golemanov, K., Denkov, N. D., Judat, S., Engel, R., & Danner, T. (2011). Efficient Emulsification of Viscous Oils at High Drop Volume Fraction. *Langmuir*, *27*(24), 14783–14796. <https://doi.org/10.1021/la203474b>

Wallecan, J., McCrae, C., Debon, S. J. J., Dong, J., & Mazoyer, J. (2015). Emulsifying and stabilizing properties of functionalized orange pulp fibers. *Food Hydrocolloids*, *47*, 115–123. <https://doi.org/10.1016/j.foodhyd.2015.01.009>

Whitesides, T. H., & Ross, D. S. (1995). Experimental and Theoretical Analysis of the Limited Coalescence Process: Stepwise Limited Coalescence. *Journal of Colloid and Interface Science*, *169*(1), 48–59.

<https://doi.org/http://dx.doi.org/10.1006/jcis.1995.1005>

Wiley, R. M. (1954). Limited coalescence of oil droplets in coarse oil-in-water emulsions. *Journal of Colloid Science*, 9(5), 427–437. [https://doi.org/10.1016/0095-8522\(54\)90030-6](https://doi.org/10.1016/0095-8522(54)90030-6)

Yusoff, A., & Murray, B. S. (2011). Modified starch granules as particle-stabilizers of oil-in-water emulsions. *Food Hydrocolloids*, 25(1), 42–55.

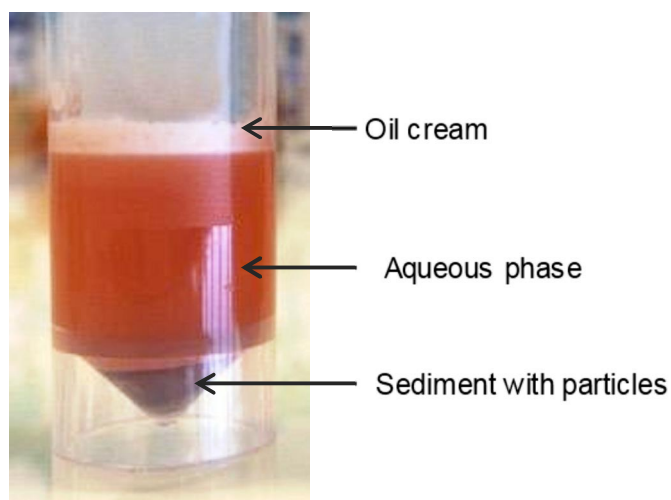
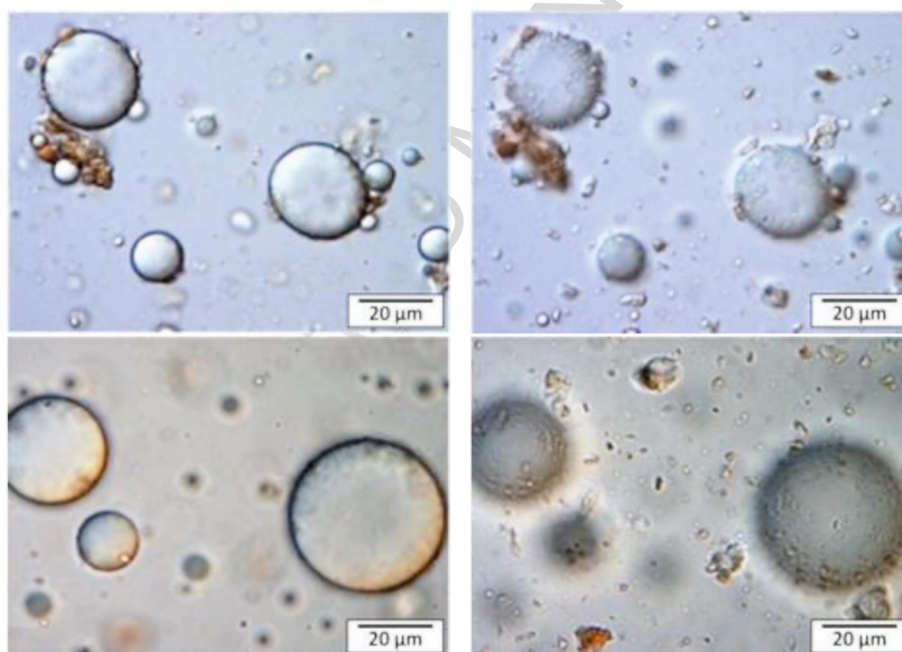
Zak, D. L., & Keeney, P. G. (1976). Extraction and fractionation of cocoa proteins as applied to several varieties of cocoa beans. *Journal of Agricultural and Food Chemistry*, 24(3), 479–483.

Zhang, Q., Zhang, J., Shen, J., Silva, A., Dennis, D. A., Barrow, C. J., & others. (2006). A simple 96-well microplate method for estimation of total polyphenol content in seaweeds.

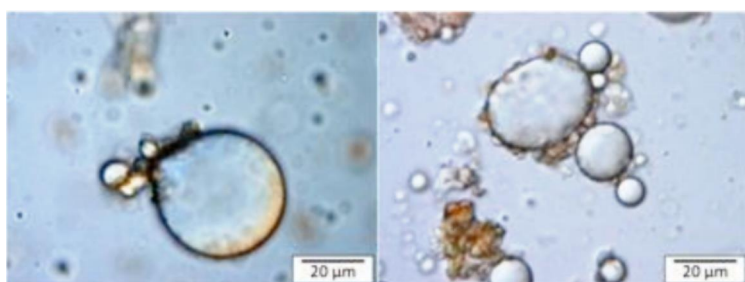
Supplementary Information

SI.1 Table indicating the composition of the emulsions discussed in this article.

Oil content		Aqueous phase content		Powder content		Emulsification process
wt. % of the whole emulsion	Mass (g)	wt. % of the whole emulsion	Mass (g)	wt. % of the aqueous phase	Mass (g)	
20	4	80	16	2.5	0.4	Ultra-Turrax [®]
20	4	80	16	2.5	0.4	Ultrasounds
20	4	80	16	2.5	0.4	Microfluidization (800 bars)
20	4	80	16	2.0 % (insoluble fraction)	0.32	Microfluidization (800 bars)
20	4	80	16	0.5 % (soluble fraction)	0.08	Microfluidization (800 bars)
20	4	80	16	1.75 % (coarse fraction)	0.28	Microfluidization (800 bars)
20	4	80	16	0.25 % (fine fraction)	0.04	Microfluidization (800 bars)
20	4	80	16	2.5	0.4	Microfluidization (500 bars)
20	4	80	16	2.5	0.4	Microfluidization (240 bars)
20	4	80	16	2.5 (pre-milled powder)	0.4	Microfluidization (240 bars)
20	4	80	16	1	0.16	Microfluidization (800 bars)
20	4	80	16	1.9	0.3	Microfluidization (800 bars)
20	4	80	16	2.5	0.4	Microfluidization (800 bars)
20	4	80	16	4	0.64	Microfluidization (800 bars)
20	4	80	16	7	1.12	Microfluidization (800 bars)
20	4	80	16	10	1.6	Microfluidization (800 bars)
20	4	80	16	15	2.4	Microfluidization (800 bars)
30	6	70	14	1	0.14	Microfluidization (800 bars)
30	6	70	14	2.5	0.35	Microfluidization (800 bars)
30	6	70	14	5	0.7	Microfluidization (800 bars)
30	6	70	14	7	0.98	Microfluidization (800 bars)
30	6	70	14	12	1.68	Microfluidization (800 bars)
10	2	90	18	0.5	0.09	Microfluidization (800 bars)
10	2	90	18	1	0.18	Microfluidization (800 bars)
10	2	90	18	1.6	0.29	Microfluidization (800 bars)
10	2	90	18	2.5	0.45	Microfluidization (800 bars)
10	2	90	18	3.3	0.59	Microfluidization (800 bars)
50	10	50	10	3	0.3	Microfluidization (800 bars)
40	8	60	12	2.5	0.3	Microfluidization (800 bars)
30	6	70	14	2.14	0.3	Microfluidization (800 bars)
15	3	85	17	1.8	0.3	Microfluidization (800 bars)
10	2	90	18	1.7	0.3	Microfluidization (800 bars)

SI.2 Particles desorption by SDS*SI.3 Micrographs of Cocoa-stabilized emulsions prepared by ultra-Thurax and ultrasounds*

Microscopic observations of a 15% cocoa particles emulsion obtained with the Ultra-Turrax® process. The objective is focused on the equatorial plane of the droplets (a) and on free particles (b)

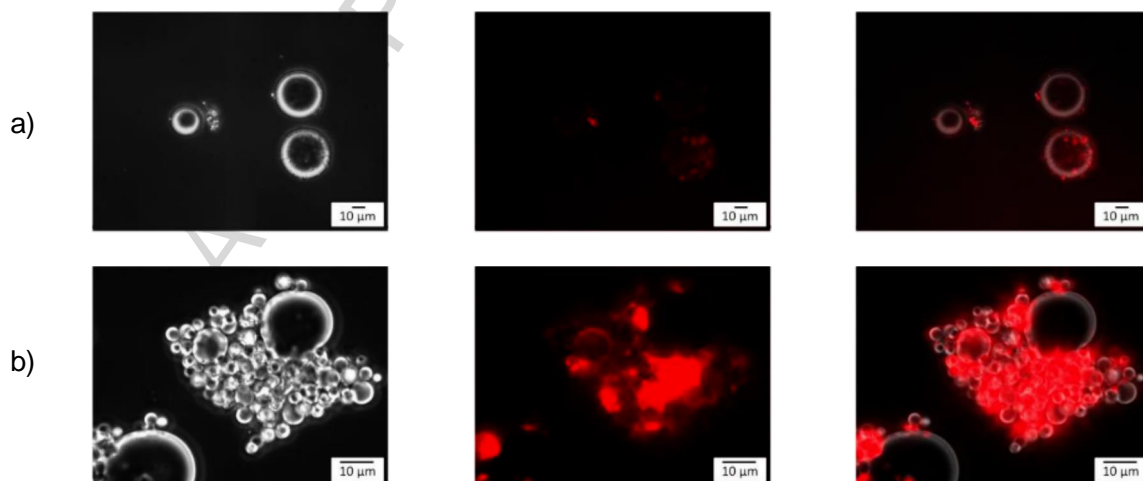


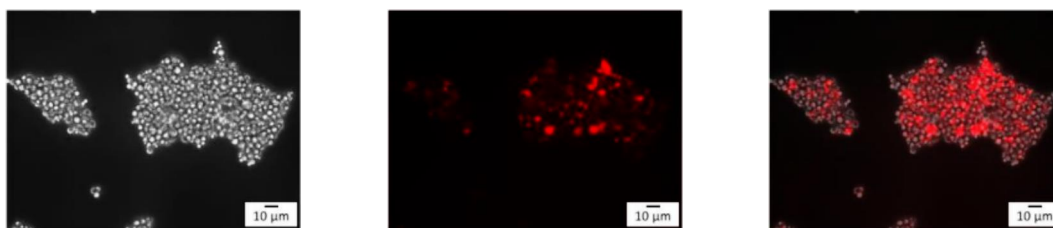
Observation of cocoa particles anchored to the oil droplets interfaces.



Emulsion composed of 2.5 wt% cocoa powder and 20 wt % sunflower oil fabricated by ultrasounds.

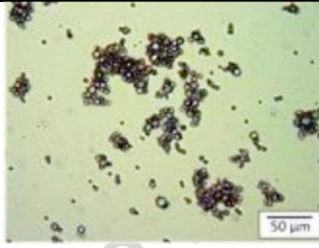
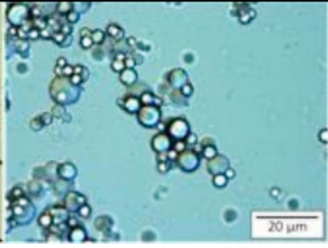
SI.4 Fluorescence microscopy of emulsions processed by microfluidization using fine or coarse particles only





Phase contrast microscopic images (left column), fluorescence microscopic images (middle) and overlay of both images (right column) of emulsions processed by microfluidization using (a) 0.25 wt.% of fine particles, (b) 1.75 wt.% of coarse particles, both without the soluble fraction.

SI.5 Microscopic images and size distribution of and emulsion fabricated with 2.5 wt.% of fine particles only

Conditions	2.5 wt.% fine particles, 20 wt.% oil, 800 bars	
Microscopy		
D_v / P	7 μ m / 0.37	

SI.6 Creaming behavior of emulsion with increasing oil content. Observations were performed 30 days after emulsion fabrication

